

# TURBULENT SIMULATION OF FLOW IN OPEN CHANNEL WITH ONE FLOODPLAIN AT $Re = 15000$

Rawya Monir Kansoh

Hydraulics and Irrigation Engineering Department, Faculty of Engineering,  
Alexandria University, Alexandria, Egypt.

## ABSTRACT

With the availability of modern technology, it is now possible to integrate numerically the Navier-Stokes equations and simulate three dimensional flow in open channels. A numerical technique for simulating turbulent flows in an open channel with one flood plain at Reynolds number of 15000 has been applied. The results were good and showed eddy existence and separation.

**Keywords:** Compound channel flow, turbulent channel flow, floodplain, flow at low Reynolds number, computational modelling.

## 1. INTRODUCTION

The turbulent motion of a liquid at a surface is much less understood than the corresponding motions at a solid boundary, but the practical applications are equally important. For example, the dispersion of pollutants in rivers and coastal waters is governed by surface phenomena. It is natural to turn to direct numerical simulation of the turbulence, and this approach is able to produce data that is more complete and often more accurate than experiments for near wall boundary layers but is limited to low Reynolds numbers. The Large Eddy Simulation approach is closely related to direct numerical simulation but rotation only the large eddies or grid scales with the smaller eddies or sub-grid scales being represented by a subgrid model. The method thus has the disadvantage of being dependent on a model but experience has shown that the dependence is much less severe than for other methods such as  $k-\epsilon$  or algebraic stress models. The large eddy simulation approach is able to extend the Reynolds number of a simulation without increasing the computational resources required. A review of numerical simulation is given by Rogallo & Moin (1984), and some recent simulations of channel flow are given by Kim, Moin & Moser (1985) and Ral & Moin (1991).

## 2. COMPUTATIONAL DOMAIN

We consider the turbulent flow of an incompressible fluid of kinematic viscosity  $\nu$  maintained by gravity in an infinite open channel of depth  $d$ . The cartesian coordinates  $(x,y,z)$  are aligned with the channel and dimensions as shown in Figure (1). The channel slopes at a small angle  $\alpha$  relative to the horizontal so that the flow is maintained with mean bed stress  $\tau_b = \frac{1}{2} U_r^2$  at the floodplain, whereas  $\tau_b \sim 1.3 U_r^2$  at the channel bottom, where  $U_r$  denotes the characteristic shear velocity  $(\alpha Rg)^{1/2}$ , and  $g$  denotes the acceleration due to gravity.

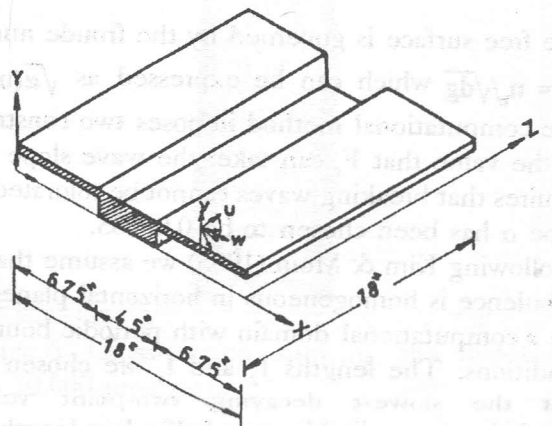


Figure 1. Channel dimensions.

The two characteristic lengths for this flow are the depth and the viscous length  $\nu/U_r$  which governs the structure of the flow near the bed.

The Reynolds number  $Re = 4R ub/\tau$  based on average velocity over the area = 1ft./sec. = 30.48 cm/sec., and the channel depth is given by  $(U_b/U_r)$  Re where  $U_b/U_r$  is determined from the simulation  $U_r = 0.011$  m/s.,  $h^+ = hu_r/\nu$ ,  $\Delta x^+ = \Delta x U_r/\nu$ . The mesh distribution has been chosen such that: 15 elements in uniform distribution in the floodplain  $y(1)=...=y(15)$ , and 35 elements of non-uniform distribution such that  $y(n+1)=y(n) \cdot \text{const.}$  starting from  $y(16)$ . In the horizontal direction, the domain is divided uniformly  $x(n+1)=x(n) \cdot [n=1,64]$ . In the Z-direction the domain has been divided into 96 elements in each side of the floodplain, and 63 elements in the channel. Figure (2) outlines the channel cross-section with the mesh distribution such as 64 50 255.

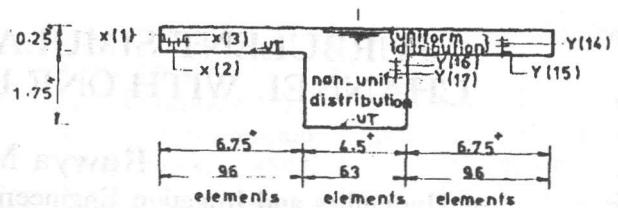


Figure 2. Channel cross-section and mesh distribution.

### 3. NUMERICAL TECHNIQUE

The velocity field  $U_1 = (u,v,w)$  satisfies a discretized form of the Navier-Stokes equations and the surface elevation  $h$  satisfies  $\partial h/\partial t = G$  where  $G$  is defined below. We use second order finite differences on a staggered mesh with an unstructured volume of fluid type treatment at the free surface. The convection terms are approximated by central difference type operators which conserve total momentum and kinetic energy in the presence of arbitrary surface deformations.

$$\Delta x = \frac{18}{64} = 0.2813'' = 0.0117' = 3.572 \times 10^{-3} \text{m}$$

$$\Delta x^* = \frac{3.572 \times 10^{-3} \times 0.011}{1 \times 10^{-6}}$$

$$\Delta y_f = \frac{0.25}{15} = 1.67 \times 10^{-2} \text{in.} = 39.3 \times \frac{1.67 \times 10^{-2}}{0.2813} = 2.3^+$$

$$\Delta y_{m/c} = \frac{1.75}{35} = 0.05 \text{in} = 39.3 \times \frac{0.05}{0.2813} = 7.0^+$$

$$\Delta z = \frac{18}{255} = 7.06 \times 10^{-2} \text{in} = 39.3 \times \frac{7.06 \times 10^{-2}}{0.2813} = 9.9^+$$

The free surface is governed by the froude number  $F_r = u_f/\sqrt{dg}$  which can be expressed as  $\sqrt{\alpha}(u_f/u_r)$ . The computational method imposes two constraints on the value that  $F_r$  can take: the wave slope limit requires that breaking waves cannot be tolerated, the slope  $\alpha$  has been chosen to be 0.00085.

Following Kim & Moin (1985) we assume that the turbulence is homogeneous in horizontal planes and use a computational domain with periodic boundary conditions. The lengths  $L_z$  and  $L_v$  are chosen such that the slowest decaying two-point velocity correlation is negligible over half a box length.

$$G_i^n = \left[ - \int_0^h \left( \frac{\delta u}{\delta x} + \frac{\delta v}{\delta y} \right) dz \right]^n$$

$$H_i^n = \left[ - \frac{\delta u_i \cdot u_j}{\delta x_j} + \nu D^2 u_i + g_i \right]^n$$

where  $n$  denotes the discrete time, level,  $\delta$  the finite difference operator,  $D^2$  the discrete Laplacian. The time advancement scheme used originally was only first order accurate and although it conserved the potential energy of surface waves it proved to be unsuitable for simulating turbulence. We require that the time truncation error associated with the convection terms be very small compared with the viscous dissipation term, and this could be satisfied only for unacceptably small time steps.

$$\frac{\hat{u}_i - u_i^n}{\Delta t} = \frac{3}{2} H_i^n - \frac{1}{2} H_i^{n-1} + \frac{1}{2} \frac{\delta p^{n-1}}{\delta x_i} \quad (1)$$

$$\frac{u_i^{n+1} - \hat{u}_i}{\delta t} = - \frac{3 \delta p^n}{2 \delta x_i}$$

$$D^2 p^n = \frac{2 \delta \hat{u}_j}{3 \Delta t \delta x_j}$$

$$\frac{h^{n+1} - h^n}{\Delta t} = \frac{1}{2} G^{n+1} + \frac{1}{2} G^n$$

where  $\hat{u}_i$  denotes an intermediate variable. The continuity equation  $\delta u_j^{n+1} / \delta x_j = 0$  is enforced at time level  $n+1$ . First,  $\hat{u}_i$  is computed using (1) and then  $p^n$  is determined such that  $u_i^{n+1}$  satisfies continuity by solving (3). The boundary conditions are assumed built into the difference operators and need not be explicitly treated. The thickness of the layer is an integral measure of the eddy size.

#### 4. MODEL RESULTS

After running the model with respect to time, it has been found that eddies and separation at the floodplain and channel intersection, also velocity vectors had apparent values in all directions.

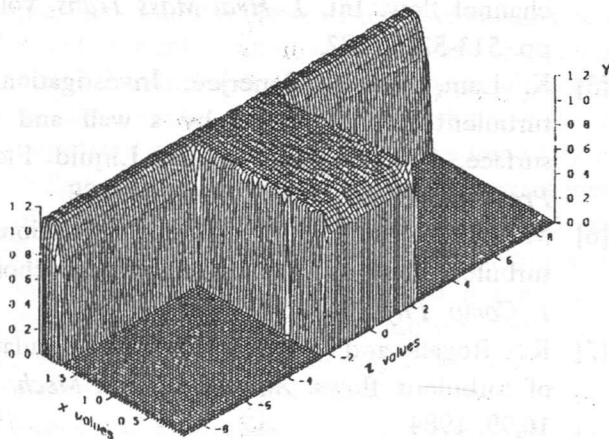


Figure 3. Velocity distribution after 4000 time steps.

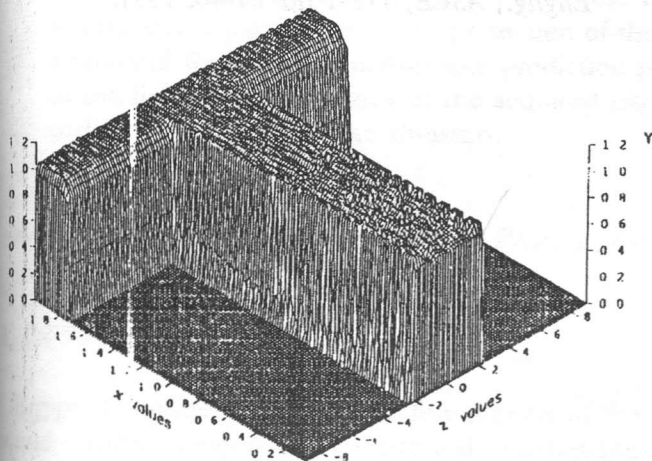


Figure 4. Velocity distribution after 8000 time steps.

Figure (3) shows the velocity distribution after 4000 time step, while Figure (4) shows the velocities after 8000 time steps showing bending of the profile in the channel bottom. Figure (5) outlines definite velocities and some separation along the intersection after 20,000 time step, while Figure (6) describes this situation in a cross-section. Finally, after 40,000 time steps, Figure (7) shows the final profile with eddy separation and velocities which is also described in cross-section profile in Figure (8).

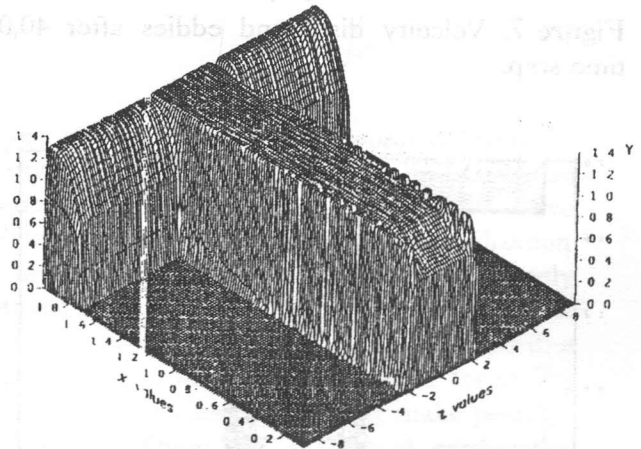


Figure 5. Velocity distribution after 20,000 time steps.

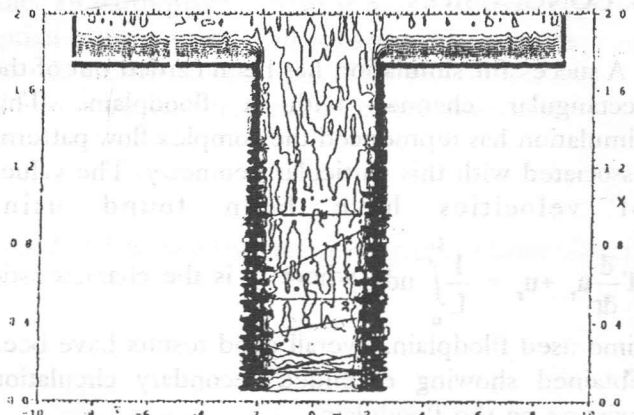


Figure 6. Cross-section showing the distribution after 20,000 time step.

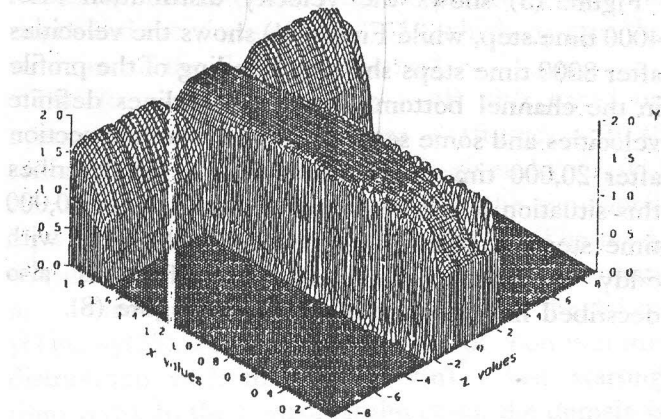


Figure 7. Velocity distr. and eddies after 40,000 time step.

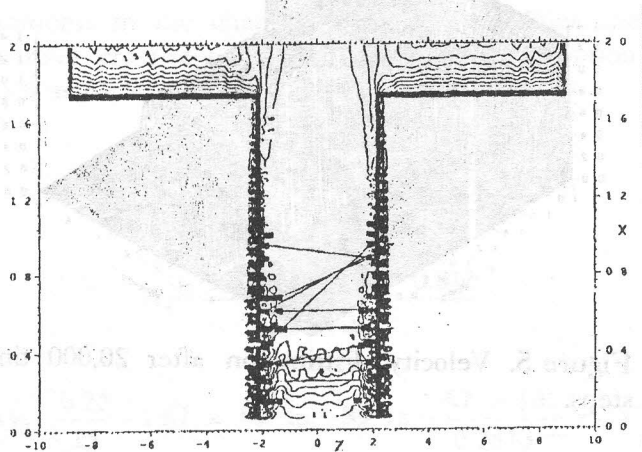


Figure 8. Final vel. distr. and separation in the cross-section.

## 5. CONCLUSION

A successful simulation has been carried out of the rectangular channel with a floodplain. This simulation has reproduced the complex flow patterns associated with this particular geometry. The values of velocities have been found using

$$T \frac{d}{dt} u_r + u_r = \frac{1}{L} \int_0^L u dx$$

where T is the characteristic

time used floodplain, overall good results have been obtained showing extended secondary circulation existing on the floodplain.

## 6. REFERENCES

- [1] H. Eckelmann, The structure of the viscous sublayer and the adjacent wall region in a turbulent channel flow. *J. Fluid Mech.* 65. 439, 1974.
- [2] J. Kim, P. Moin, and R. Moser, Turbulence statics in fully developed flow at low Reynolds number, *J. Fluid Mech.* 177. pp. 133-166, 1985.
- [3] D.W. Knight and J.D. Demetrios, Floodplain and main channel flow interaction, *J. Hydr. Engng., ASCE*, 109-8, pp. 1073-1092, 1983.
- [4] S. Komori, H. Ueda, F. Ogino and T. Mizushima, Turbulence structure and transport mechanism at the free surface in an open channel flow. *Int. J. Heat Mass Trans.* vol 26. pp. 513-521, 1982.
- [5] K. Lam, and S. Banerjee, Investigation of turbulent flow bounded by a wall and free surface. *Fundamentals of Gas-Liquid Flows, Proc. ASME Ann. Mtg., Chicago*, 1988.
- [6] M.M. RAI, and P. Moin, Direct simulations of turbulent flow using finite difference schemes *J. Comp. Phys.* 96, 15-53, 1991.
- [7] R.S. Rogallo and P. Moin, Numerical simulation of turbulent flows. *Ann Rev. Fluid Mech.* vol. 16, 99, 1984.
- [8] A. Tominaga, and I. Nezu, Turbulent Structure in compound open channel flows. *J. Hydr. Engng., ASCE*, 117-1 pp. 21-40, 1991.